

Lattice disorder and electrical conductivity of flux-grown $\text{Ca}(\text{WO}_4)_x(\text{MoO}_4)_{1-x}$ crystals

S. K. ARORA, R. S. GODBOLE, D. LAKSHMINARAYANA

Department of Physics, Sardar Patel University, Vallabh Vidyanagar 388 120, Gujarat, India

The growth of solid solutions of $\text{Ca}(\text{WO}_4)_x(\text{MoO}_4)_{1-x}$ in the range $x = 0.072$ to 0.86 has been successfully accomplished for the first time, employing a flux technique. The fact that proper mixing occurs is established by observing the variation in unit cell parameters and density of the crystals. The electrical conductivity of the pelletized samples is interpreted in terms of Schottky and Frenkel defect concentrations. The role of oxygen ion vacancies is stressed for the intrinsic region of conductivity.

1. Introduction

Although available literature supplies enough information about the electrical conduction in alkali halides [1-5] and rare earth tungstates such as $\text{Nd}_2(\text{WO}_4)_3$ and EuWO_4 [6-8] where the conductivity is interpreted as due to electrons (or holes), polarons and impurities, a meagre amount of literature is recorded about mixed scheelite compounds. Rigdon and Grace [9] and Lal *et al.* [10] have, to some extent, investigated the electrical conductivity of CaWO_4 crystals. The presence of oxygen vacancies helped Van Loo [11] to explain the conductivity of PbMoO_4 and PbWO_4 crystals.

The electrical conductivity essentially projects the role of imperfections, since in real crystals the electrons collide with dislocations, vacancies and other defects, e.g. lattice phonons. The study of conductivity of the laboratory grown $\text{Ca}(\text{WO}_4)_x(\text{MoO}_4)_{1-x}$ mixed crystals, in association with their thermal behaviour, is reported here, which helps to quantify the lattice defect mechanism. This is the first time that the crystal growth of a complete series of mixed configurations of tungstates and molybdates of calcium has been reported herein.

2. Experimental details

2.1. Crystal growth

First, the solubility of CaWO_4 and CaMoO_4 in molten LiCl was determined at different temperatures in the range 600 to 900°C by

the supersaturation method. Then, single crystal growth of the series of mixed compounds $\text{Ca}(\text{WO}_4)_x(\text{MoO}_4)_{1-x}$, with $x = 0.072$, to $x = 0.86$, was attempted from the unstirred melts of LiCl , employing the conventional slow cooling flux technique. The growth procedure is summarized as follows. Proper amounts of the solute ($\text{CaMoO}_4 + \text{CaWO}_4$) and the solvent LiCl were accurately weighed, thoroughly mixed with a small quantity of NaCl (which serves to suppress the high evaporation of LiCl and hence to improve the quality of growing crystals), and packed into a 100 cc platinum crucible covered with a loosely fitting lid. The charge was placed in the vertical tube of a muffle furnace, the temperature raised up to 850°C and held there for 2 h . The furnace was then suddenly brought down to 750°C and a slow cooling of 3°C h^{-1} was carried out down to 550°C , after which the input power was switched off. The crystals were leached out by washing the residual flux with hot distilled water. Three or four runs of crystal growth were made for each composition of the mixed series.

Well faceted and transparent single crystals with maximum size 7 mm were grown. The crystals, when examined by "Epignost" optical microscope, were found to be tetragonal bipyramids bounded by prominent (011) faces. Their unit cell parameters, a and c , were evaluated by choosing 2θ angles of (200) and (004) reflections in the X-ray powder diffractograms. Their average densities were determined pycnometrically. Their

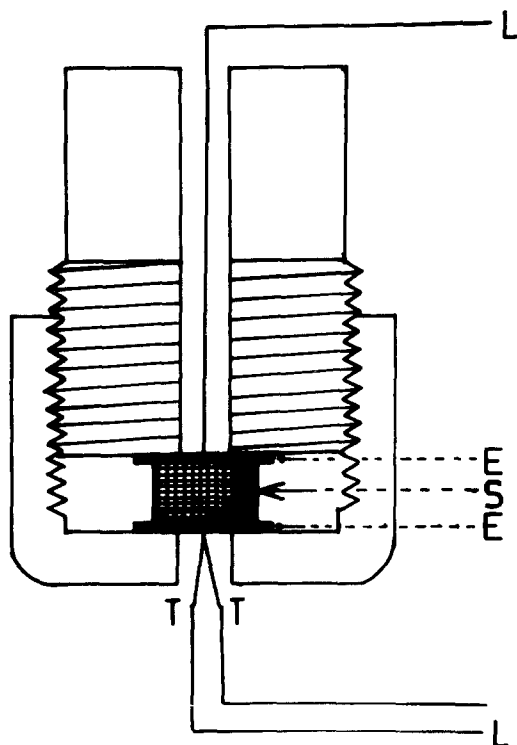


Figure 1 Schematic diagram of the conductivity cell. L – connecting leads, E – platinum electrodes, S – sample pellet, T – thermocouple leads.

unit cell volume and hence their X-ray density were computed theoretically, according to Vegard's law. The difference between the experimental and the theoretical values of the density, which is a measure of the difference in packing, helped us to estimate the Schottky defects in crystals.

2.2. Conductivity measurements

The geometrical nonuniform morphology of crystals, coupled with the requirement of large areas of contact, made it necessary to powder the crystals for conductivity measurements. The fine powder was pelletized at a constant pressure of 15 000 psi*, using a suitable die in a hydraulic press. The dimensions of pellets were 3 mm thickness and 10 mm diameter, with their packing density being 85 to 87% of that of the parent crystals. A porcelain conductivity cell was specially fabricated which is schematically displayed in Fig. 1. It consists essentially of a pair of 1 mm thick electrodes made of pure platinum connected to platinum leads. The pellet with smooth surfaces was carefully mounted between the two flat

TABLE I Activation and Frenkel defect formation energies in eV for $\text{Ca}(\text{WO}_4)_x(\text{MoO}_4)_{1-x}$ series and concentration of Frenkel defects n_F per unit cell

Composition	E_1	E_2	h_F	n_F
$x = 0$	1.72	0.67	1.05	9.4×10^{-4}
$x = 0.23$	1.90	0.86	1.04	1×10^{-3}
$x = 0.41$	1.94	0.99	0.95	2.1×10^{-3}
$x = 0.62$	2.20	0.78	1.42	4.4×10^{-5}
$x = 0.86$	2.13	0.72	1.41	4.7×10^{-5}
$x = 1$	1.35	0.615	0.735	1.3×10^{-2}

electrodes. The screwable upper part of the cell ensured perfect tightening and good specimen contact. The specimen temperature was monitored by means of a 13% Pt/Pt–Rh thermocouple connected to the lower electrode. The cell was placed in a resistance heated furnace, and the temperature of the sample was increased by regulating, through a “dimmerstat”, the input power of the furnace. The resistivity was measured in the temperature interval of 300 to 900 K, using BPL (India) million megohmmeter with an accuracy of $\pm 5\%$. The samples were studied above 100°C to avoid the effect of surface moisture, if any. However, one cannot afford to rule out a possibility of significant surface conduction occurring on the extensive internal surface of the pellets, which would yield, as is widely recognised, only qualitative irreproducible results. With a view to removing the possible errors due to the internal surface conduction, the pellets were subjected to heating and cooling for three or four cycles, prior to the conductivity measurements. That the repeated heating and cooling, rather than heating at high temperature, results in reproducible data, as has been successfully accomplished by Lal *et al.* [10] and Van Loo [11], is due to settlement of various granules of the pellets. Consequently, the quantitative data presented in Table I, Section 3, are far from speculative. The reproducible values of σ have been taken as the bulk values of the solid.

3. Results and discussion

The experimental pycnometric, and the theoretically calculated X-ray, densities of the complete range of mixed compositions are graphically depicted in Fig. 2. The lowest curve depicts the increment in the pycnometric density, $(\Delta\rho/\rho)_{\text{exp}}$, with increase of x . These observations reveal that there is a proper growth of the substantial solid solutions, the WO_4^{2-} ions regularly replacing the

*1 psi = 6.89×10^3 Pa.

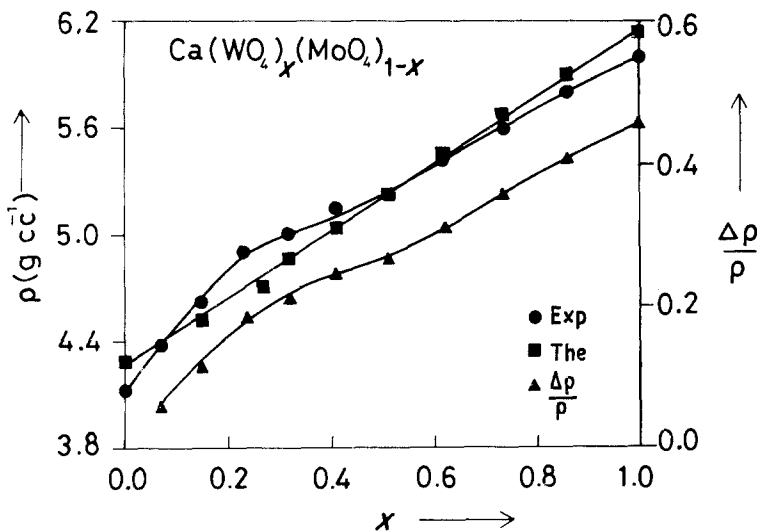


Figure 2 Graph of density against composition x .

MoO_4^{2-} ions in the CaMoO_4 lattice. This was doubtlessly, expected because of the isostructural matrices of CaWO_4 and CaMoO_4 and their well-fitting ionic radii. Further, the systematic deviation in the observed density with respect to the X-ray density for each value of x was worked out to give the mole per cent of Schottky defects, $C = (\Delta\rho/\rho) \times 100\%$, which are graphically shown in Fig. 3. It may be remarked that while $\Delta\rho/\rho$ in Fig. 2 corresponds to experimental packing deviation, $\Delta\rho/\rho$ in Fig. 3 corresponds to packing differences between experimental and theoretical values, ρ being chosen for CaMoO_4 . The values of the random entropy, ΔS_{rand} , were computed using the formula

$$\Delta S_{\text{rand}} = -R(C_1 \log C_1 + C_2 \log C_2) \quad (1)$$

where R is the gas constant, and C_1 and C_2 are the concentrations of WO_4 and MoO_4 components, respectively, which have been plotted in Fig. 4.

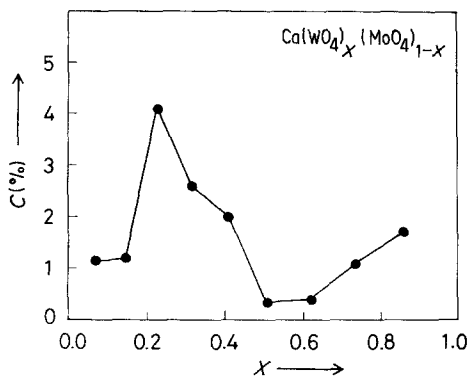


Figure 3 Graph of Schottky defect concentration C (%) against composition x .

Taking into consideration the concentration of vacancies, the configurational entropy ΔS_{conf} , as thought of by Makarov *et al.* [12] has been calculated using the following relation:

$$\Delta S_{\text{conf}} = -R \left[(1+C) \left(\frac{C_1}{1+C} \right) \log \left(\frac{C_2}{1+C} \right) + \left(\frac{C_2}{1+C} \right) \log \left(\frac{C_2}{1+C} \right) + 2C \log C + (1-C) \log (1-C) \right] \quad (2)$$

where C represents the mole fraction of vacancies, either cation or anion, in the lattice. The results obtained as a function of x are graphically shown in Fig. 4. Evidently, the two entropy curves showed by dotted and continuous lines do not seem to be much different. Nevertheless, the configurational entropy, ΔS_{conf} , is taken in general, to be a better representative of the lattice disorder, because of the involvement of Schottky defects, in the mixed crystals. It is noteworthy that the entropy, and hence the lattice disorder, changes substantially throughout the range of compositions, being maximum at the almost equimolar mid-composition, namely, $\text{Ca}(\text{WO}_4)_{0.51}(\text{MoO}_4)_{0.49}$.

The variation in the experimental values of conductivity, $\sigma(x)$, at some chosen temperatures from the range 400 to 700 K is illustrated in Fig. 5. It is particularly difficult to analyse the observed variation for want of the knowledge of the structure of energy bands in the crystal configurations. Nonetheless, one is of the opinion

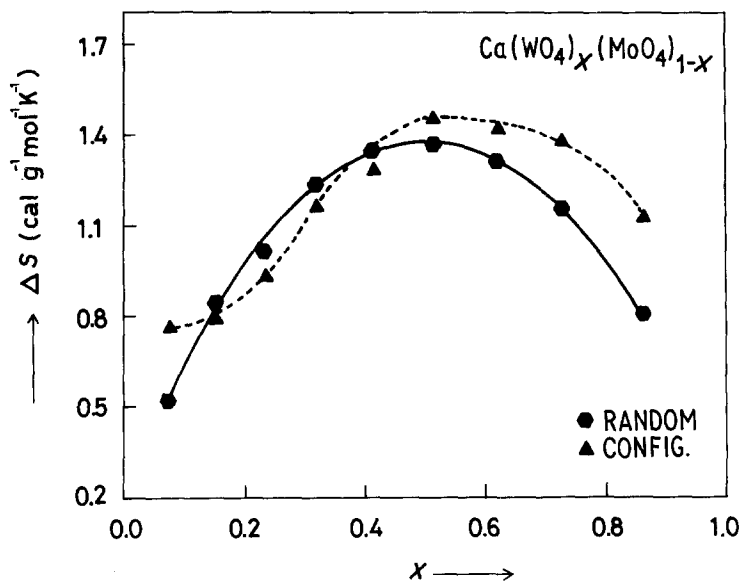


Figure 4 Graph of entropy against composition x .

that except for the variation between $x = 0.86$ and $x = 1.0$, the general conductivity in the entire temperature spectrum falls to around the mid-composition and increases thereafter. The "misbehaviour" beyond $x = 0.86$ is not understood.

The results of conductivity at different temperatures are far more interesting. The variation of $\ln \sigma T$ with the reciprocal of temperature is depicted in Fig. 6. The values for the end partners, namely CaMoO_4 and CaWO_4 , and one of the

mixed varieties, namely, $\text{Ca}(\text{WO}_4)_{0.41}(\text{MoO}_4)_{0.59}$, have been plotted to understand the general conductivity behaviour of the mixed ionic species.

It is to be noted that the slopes of the curves change from 570 to 610 K for CaWO_4 to CaMoO_4 , respectively, through the intermediate values for mixed species. These temperatures demarcate the two conductivities contribution by the two different types of charge carriers. One is inclined to believe that the two slopes in Fig. 6 are responsible for the intrinsic conductivity at lower temperatures

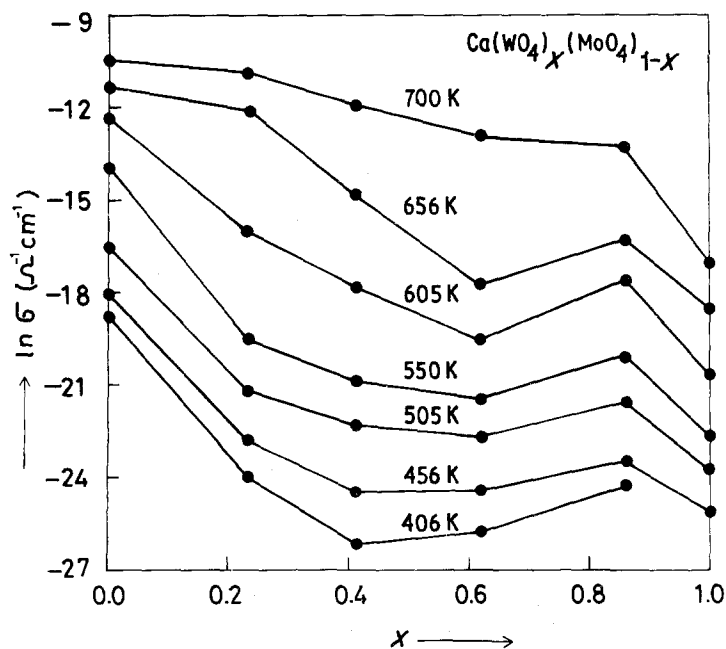


Figure 5 Graph representing $\ln \sigma$ against composition x at temperature 400 to 700 K.

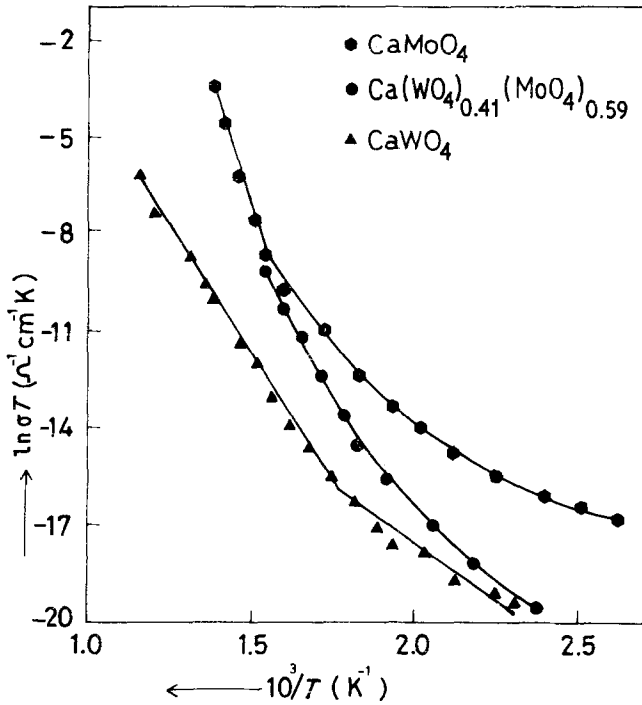


Figure 6 Graph representing $\ln \sigma T$ against $10^3/T$ for various crystals.

(400 to 600 K), both being independent of the specimen preparation history [13]. It is also evident from Fig. 6 that throughout the temperature range studied, CaMoO_4 conducts more than CaWO_4 .

The conductivity corresponding to the high temperature region (> 600 K) is expressed by

$$\sigma T = A_1 \exp\left(-\frac{E_1}{kT}\right) \quad (3)$$

with

$$E_1 = \frac{1}{2} h_F + h_m \quad (4)$$

where h_F is the energy of formation of Frenkel defects and h_m is the migration energy of the mobile species and A_1 is the pre-exponential constant.

At low temperatures (< 600 K), the conductivity, being determined by the frozen-in defects, is given by

$$\sigma T = A_2 \exp\left(-\frac{E_2}{kT}\right) \quad (5)$$

where

$$E_2 = h_m \quad (6)$$

and A_2 is another pre-exponential factor. Should the same carrier be mobile in the two temperature regions, the Frenkel defect formation energy

h_F can be computed from Equations 4 and 6 as

$$h_F = 2(E_1 - E_2) \quad (7)$$

The activation energies E_1 and E_2 , calculated from the two slopes are presented along with Frenkel defect formation energy of each of the different crystal compositions, in Table I. The number of Frenkel defects per unit cell, n_F has also been worked out according to the relation

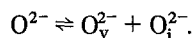
$$n_F = (NN_i)^{1/2} \exp(-h_F/2kT) \quad (8)$$

and given in Table I. Here N and N_i represent the concentration of lattice points and interstitial sites, respectively. It is essentially implied that the activation enthalpy of the low temperature conductivity region is lower than the one of the high temperature conductivity.

3.1. Intrinsic region

In ionic crystals there are two kinds of Frenkel defects, accentuated by cations or anions moving into interstitial positions [14]. The motion of the interstitial ions and the vacant lattice points constitute a current. Now since the ionic sizes of Ca^{2+} and WO_4^{2-} or MoO_4^{2-} are different, we expect a large difference in the energies required to put them into interstitial positions. Hence, in such a crystal where the current is due to Frenkel defects, either the anions or the cations only will be

responsible for conduction phenomena. The experiments on reduction of CaWO_4 by Nassau and Loiacono [15] and on annealing of PbWO_4 by Van Loo [11] help us to believe that the oxygen might be highly mobile in scheelites at high temperatures. Also, the fact that Frenkel and anti-Frenkel disorder exist in CaWO_4 lattices, as verified by Rigdon and Grace [9], supports the formation of oxygen ion vacancies O_v^{2-} and interstitials O_i^{2-} by the reaction,



Hence, it is the migration of the thermally activated defects in the tetraoxide sublattice that contributes significantly to the conductivity at higher temperatures. Further, with respect to the oxygen ion stability, calcium tungstate is relatively more stable than any molybdates, the latter losing oxygen more easily, as observed by Van Loo [16]. Consequently, the oxygen ion vacancies which are the prominent charge carriers would be more in number in CaMoO_4 , which explains its enhanced conductivity compared to CaWO_4 .

3.2. Extrinsic region

At temperatures below 600 K, the structure sensitive ionic conductivity predominates, due to mobile ions or lattice defects. These defects move at random in absence of the external field but drift with the field applied, thereby accounting for the observed extrinsic conductivity. From the calculations of Schottky defect concentrations, depicted in Fig. 2, it is evident that some amount of Schottky defects are frozen in the crystals during their growth.

4. Conclusions

1. The substitutional solid solutions of $\text{Ca}(\text{WO}_4)_x(\text{MoO}_4)_{1-x}$ in the range $x = 0.072$ to 0.86 are successfully grown by slowly cooling the polycomponent system, $\text{CaWO}_4:\text{CaMoO}_4:\text{LiCl}:\text{NaCl}$.

2. During growth of the mixed single crystals, some amount of Schottky defects gets frozen-in.

3. The electrical conductivity of CaMoO_4 is higher than that of CaWO_4 crystals, and the

mixed crystals conduct within these two boundaries, throughout the temperature interval of 400 to 700 K.

4. Intrinsic conductivity in these crystals, above around 600 K, is due to oxygen ion vacancies, whereas the extrinsic region is attributed to the structure-sensitive conductivity due to frozen-in defects.

Acknowledgements

One of the authors (RSG) expresses his gratitude to the UGC, New Delhi for the award of a Teacher Fellowship and the Principal, Kittel College, Dharwar for study leave. DLN thanks the UGC, New Delhi for an award of research scholarship.

References

1. J. D. ESHEBY, C. W. A. NEWEY and P. L. PRATT, *Phil. Mag.* **3** (1958) 75.
2. R. W. DREYFUS and A. S. NOWICK, *Phys. Rev.* **126** (1962) 1367.
3. S. C. JAIN and S. L. DAHAKE, *Ind. J. Pure Appl. Phys.* **2** (1964) 71.
4. K. C. KAO, L. J. GILES and J. H. CALDERWOOD, *J. Appl. Phys.* **39** (1968) 3955.
5. L. B. HARRIS, *J. Phys. Chem. Solids* **32** (1971) 59.
6. H. B. LAL and N. DAR, *ibid.* **38** (1977) 161.
7. H. B. LAL and N. DAR, *J. Phys. C: Solid State Phys.* **8** (1975) 2745.
8. H. B. LAL, N. DAR and ASHOK KUMAR, *ibid.* **7** (1974) 4335.
9. M. A. RIGDON and R. E. GRACE, *J. Amer. Ceram. Soc.* **56** (1973) 475.
10. H. B. LAL, N. DAR and ASHOK KUMAR, *Ind. J. Pure Appl. Phys.* **12** (1974) 539.
11. W. VAN LOO, *J. Solid State Chem.* **14** (1975) 359.
12. L. L. MAKAROV, B. G. LUR'E and V. N. MALYSHEV, *Fiz. Tver. Tela.* **2** (1960) 88.
13. R. BHARATI and R. A. SINGH, *J. Mater. Sci.* **16** (1981) 511.
14. N. F. MOTT and R. W. CURNEY, "Electronic Processes in Ionic Crystals" (Clarendon Press, Oxford, 1957) p. 41.
15. K. NASSAU and G. M. LOIACONO, *J. Phys. Chem. Solids* **24** (1963) 1503.
16. W. VAN LOO, PhD thesis, State University, Utrecht (1975).

Received 11 May

and accepted 4 October 1982